

Supplementary “Materials and Methods” and Results

Materials and Methods

RNA-Seq transcriptome analysis:

Fifteen μg total RNAs extracted from 4 μM SAHA-treated or non-treated H23 cells were reversed transcribed and fragmented for 150-250 base pairs DNA fragments by gel electrophoresis. Samples were subjected for short read sequencing by using next-generation sequencing (NGS) technology with SOLiD™ 4 system (Applied Biosystems). The reads were mapped to human genome (hg19) using BioScope 1.3 Whole Transcriptome Analysis Pipeline. To identify differential expressions between 2 samples, the “reads per kilobase of exon per million mapped sequence reads” (RPKM) values of the Ensembl genes were calculated using the RNA-seq workflow in the Partek® Genomics Suite™ (version 6.5, Partek Inc, St. Louis, MO, USA) for determination of expression fold changes. The list of metastasis-related genes reported previously was retrieved from searching Molecular Signatures Database (MSigDB) (1) with output of 3 metastasis-related gene sets: ALONSO_METASTASIS_EMT_UP (2), ALONSO_METASTASIS_UP (2) and NAKAMURA_METASTASIS (3).

Subcutaneous tumor xenograft formation assay:

The protocols of animal experiments was modified from previous report (4-8) and approved by the animal safety committee of Academia Sinica, Taiwan. Hep3B (2×10^6 cells per mouse) cells re-suspended in 0.2 ml phenol red-free Matrigel (BD) was subcutaneously inoculated in right flank of 4-5 weeks old male BALB/c nude mice ($n = 13$; LASC, Taipei, Taiwan) by a 24-gauge needle (Fig. 5A; Step 1). The width and length of the tumors were measured with a caliper and the tumor volume was calculated by the following formula: tumor volume = $0.5 \times (\text{width})^2 \times \text{length}$. When tumor volume reached 40~80 mm³ (Step 2), mice were divided into two groups: vehicle control ($n = 2$) and TSA ($n = 11$; 10 mg/kg/day)-treated mice via intraperitoneal injection by a 26-gauge needle daily. When therapeutic effects of TSA reached distinguishable tumor sizes of all mice in compared with that of control mice (Step 3), the mice in TSA treatment were further randomly subdivided into 3 groups: TSA ($n = 3$; 10 mg/kg/day)-treated mice, TSA/Cur ($n = 4$; Cur: 40 mg/kg/day)-treated mice and TSA/Tam ($n = 4$; Tam: 10 mg/kg/day)-treated mice. All the therapeutic drug treatments were continuous administration with therapeutic dosages reported previously. Neither therapeutic protocols cause toxicity nor significant body weight changes to the mice (Figure S6C). When therapeutic effects of combined treatments reached distinguishable tumor sizes of all mice in compared with TSA-treated mice, the mice were euthanized by CO₂ inhalation. Similarly,

H23 cells (Fig. 5B; 2×10^6 cells per mouse) were also inoculated for combination therapies with subcutaneous tumor xenograft formation assay. Similar to the abovementioned protocol, a total of 23 mice were divided into vehicle control ($n = 5$), SAHA ($n = 6$; 100 mg/kg/day)-treated, SAHA/Cur ($n = 6$; Cur: 40 mg/kg/day) and SAHA/Tam ($n = 6$; Tam: 10 mg/kg/day)-treated mice. The xenograft tissues were isolated for total protein extraction by RIPA buffer. Ten μg total protein in each sample was used for Western blot analysis.

RT-PCR:

Drugs-treated or untreated cells for 48 hr were lysed and total RNA was isolated by QIAGEN RNeasy Mini Kit (QIAGEN sciences). Four μg total RNA was reverse-transcribed to first-strand cDNA by ThermoScript RT-PCR System (Invitrogen) to a final volume of 20 μl . One μl cDNA solution from each treatment was used for PCR reactions with gene specific primer pairs and *GAPDH* as internal control (Table S2). Those PCR products were separated by 2.5% agarose gel electrophoresis and then revealed by ethidium bromide staining and imaging analyzer (Gel Doc-IT Imaging System; UVP).

Chromatin immunoprecipitation (ChIP) assay:

The materials and methods of ChIP assay were described previously (9). After 48 hr TSA treatment, the anti-acetyl-histone H3 or

H4 antibodies (Millipore) immunoprecipitated DNA fragments was purified and the promoter regions of *MMP* or *PKC* genes were PCR amplified with specific primer pairs (Table S3). The PCR products were then separated by a 2.5% agarose gel and revealed by ethidium bromide staining and imaging analyzer. The results were repeated multiple times with multiple cell extracts for data reproducibility (n ≥ 3).

PKC activity assay:

Twenty µg of Hep3B protein extracts from TSA and/or PKCi (Bis, Cur or Tam) treatments was applied for analysis of total PKC activity by PKC kinase activity assay kit (Assay designs). TSA monotreatment is for 48 hr treatment. Combination treatments were firstly treated with TSA for 24 hr and then followed by TSA/PKCi treatment for another 24 hr. Total native protein lysates of treated or untreated cells were extracted by phosphosafe extraction reagent (EMD Bioscience) and quantified by BCA protein assay kit. Each treatment was done in triplicate.

Western blot analysis:

In experiments of TSA monotreatment, Hep3B cells were treated with TSA for 48 hr. However, in experiments of combination treatments, Hep3B cells were treated with TSA for 24 hr and then replaced with fresh media contained TSA with PKCi for another 24 hr. Treated or untreated cells were lysed and the total cellular protein was extracted by RIPA buffer. The secreted protein in

conditional serum-free media was concentrated by TCA precipitation (Sigma-Aldrich). The protein concentration was analyzed by BCA protein assay kit (Pierce Chemical). Twenty μg protein from various treatments was separated by 8~12 % SDS-PAGE gel and then transferred onto PVDF membranes (Millipore). Membranes were then probed with specific antibodies (Table S4) at room temperature for 2 hr. Membranes were then washed with TBST and re-probed with anti-goat (Santa Cruz), mouse or rabbit (abcam) IgG HRP conjugate antibodies (1:10000) at room temperature for 1 hr. The signal on membranes was revealed by enhanced chemiluminescence reagents (SuperSignal, Pierce Chemical) and film autoradiography (Kodak Rochester, NY).

Experimental metastasis assay:

The experiment was modified from previous report (5-8, 10). To reveal the metastatic tumor cells in nude mice through labeling of green or red fluorescence protein (GFP or RFP) (Clontech Laboratories, CA, USA), we transfected the pEGFP-C1 plasmid into H23 cells (H23-GFP) and pDsRed2-C1 plasmid into Hep3B (Hep3B-RFP) and H928 (H928-RFP) cells by lipofectamine 2000 transfection reagent and selected by G418 (Invitrogen). 1×10^6 cells (H23-GFP, Hep3B-RFP or H928-RFP cells) re-suspended in 0.3 ml divalent cation-free Dulbecco's PBS (CMF-DPBS; Invitrogen) were injected into each mouse through tail vein injection with a 26-gauge needle. After tail vein injection, mice were divided into HDACi-untreated vehicle control ($n = 10\sim 16$) and HDACi-treated mice ($n = 10\sim 16$; Fig. S3). HDACi (TSA: 10 mg/kg/day; SAHA: 100 mg/kg/day or VA: 400 mg/kg/day) was simultaneously delivered to groups of HDACi-treated mice through intraperitoneal injection by a 26-gauge needle daily. After two months, all mice were euthanized by CO_2 inhalation. The lung and liver organs from those mice were isolated and rinsed with PBS. Fluorescent cells on lung or liver were revealed by fluorescence stereomicroscope (Carl Zeiss).

References:

1. Subramanian A, Tamayo P, Mootha VK, Mukherjee S, Ebert BL, Gillette MA, et al. Gene set enrichment analysis: a knowledge-based approach for interpreting genome-wide expression profiles. *Proc Natl Acad Sci U S A*. 2005;102:15545-50.
2. Alonso SR, Tracey L, Ortiz P, Perez-Gomez B, Palacios J, Pollan M, et al. A high-throughput study in melanoma identifies epithelial-mesenchymal transition as a major determinant of metastasis. *Cancer Res*. 2007;67:3450-60.
3. Nakamura T, Fidler IJ, Coombes KR. Gene expression profile of metastatic human pancreatic cancer cells depends on the organ microenvironment. *Cancer Res*. 2007;67:139-48.
4. Chuu JJ, Liu JM, Tsou MH, Huang CL, Chen CP, Wang HS, et al. Effects of paclitaxel and doxorubicin in histocultures of hepatocellular carcinomas. *J Biomed Sci*. 2007;14:233-44.
5. Tang XX, Robinson ME, Riceberg JS, Kim DY, Kung B, Titus TB, et al. Favorable neuroblastoma genes and molecular therapeutics of neuroblastoma. *Clin Cancer Res*. 2004;10:5837-44.
6. Luong QT, O'Kelly J, Braunstein GD, Hershman JM, Koeffler HP. Antitumor activity of suberoylanilide hydroxamic acid against thyroid cancer cell lines in vitro and in vivo. *Clin Cancer Res*. 2006;12:5570-7.
7. Zeisig R, Ruckerl D, Fichtner I. Reduction of tamoxifen resistance in human breast carcinomas by tamoxifen-containing liposomes in vivo. *Anticancer Drugs*. 2004;15:707-14.
8. Gururajan M, Dasu T, Shahidain S, Jennings CD, Robertson DA, Rangnekar VM, et al. Spleen tyrosine kinase (Syk), a novel target of

curcumin, is required for B lymphoma growth. *J Immunol.* 2007;178:111-21.

9. Lin KT, Yeh SH, Chen DS, Chen PJ, Jou YS. Epigenetic activation of alpha4, beta2 and beta6 integrins involved in cell migration in trichostatin A-treated Hep3B cells. *J Biomed Sci.* 2005;12:803-13.

10. Xu L, Mohanty S. Experimental Metastasis Assay. *J Vis Exp.* 2010:e1942.

Table S1. MMPs and PKCs primer pairs and PCR conditions for RT-PCR

Genes	Primer pairs	Base pairs	°C, cycles	Genes	Primer pairs	Base pairs	°C, cycles
MMP1	Fw 5'-gtactgataataattagttc-3' Rv 5'-gttatccctgcctatctag-3'	256	45,45	PKC-α	Fw 5'-cgaggaaggaaacatggaactcag-3' Rv 5'-cctgtcggcaagcatcaccttt-3'	193	60.3, 45
MMP2	Fw 5'-aacctcagagccacccta-3' Rv 5'-gtgcatacaaaagcaaacg-3'	287	62.4, 40	PKC-βI	Fw 5'-agagacaagagagacacctccaac-3' Rv 5'-gaattgatacatagcttggcttg-3'	218	55, 45
MMP3	Fw 5'-cgatgcagccatttctgata-3' Rv 5'-gtgccatattgtgccttct-3'	302	62.4, 50	PKC-βII	Fw 5'-tgtggggcaaatgctgaaaactcgaccga-3' Rv 5'-gtctcatcagaaaatcaaacatggatgcaactggc-3'	275	60.3, 45
MMP7	Fw 5'-aggagatgctcacttcgatga-3' Rv 5'-ccataggtggatacatcactgc-3'	150	55,45	PKC-γ	Fw 5'-tgtgcccgctatgtaatctc-3' Rv 5'-agtccagaacgctaaggta-3'	270	59, 35
MMP8	Fw 5'-tggcttaactgtagataggctga-3' Rv 5'-ggcttacttccctcttcttgatg-3'	270	46.8, 45	PKC-δ	Fw 5'-gcatcgccctcaactcctatgagct-3' Rv 5'-acacacccacggctcacctcaga-3'	249	65.1, 45
MMP9	Fw 5'-tgggctactgacctatgac-3' Rv 5'-caaaggtgagaagagagggc-3'	191	62.4, 45	PKC-ϵ	Fw 5'-tcaatggccttcttaagatcaaaa-3' Rv 5'-cctgagagatcgatgatcacatac-3'	388	60.3, 45
MMP10	Fw 5'-gtccttcgatgccatcagca-3' Rv 5'-cttgctccatggactggcta-3'	380	62.4, 40	PKC-η	Fw 5'-aacgaggagttttgcgctaa-3' Rv 5'-tggtaaaatgittgaagatccg-3'	262	55, 45
MMP11	Fw 5'-tcagccctggctgagcaact-3' Rv 5'-attgaggtatgtgcagcct-3'	214	62.4, 40	PKC-θ	Fw 5'-ctcgtcaagagatgtcgaatca-3' Rv 5'-aattcattcatgctcttgtgactca-3'	308	46.8, 40
MMP12	Fw 5'-gaaattgaagccagaaatcaag-3' Rv 5'-tgctttcagtgtttggta-3'	385	62.4, 40	PKC-ζ	Fw 5'-ccgagcaccctgagcagcctg-3' Rv 5'-gtcggctcctcgttctgtgctct-3'	321	62.4, 45
MMP13	Fw 5'-tgaagagcatttgggtaat-3' Rv 5'-tgtgggaagtatcatcaaccatt-3'	237	60.3, 40	PKC-ι	Fw 5'-tgtgttccctgtgtaccagaacgt-3' Rv 5'-catcactggttccctgtggcaag-3'	292	60.3, 45
MMP14	Fw 5'-ttcacagttagaagagctgaaacca-3' Rv 5'-cgtcctcatttctcttttg-3'	201	55, 40	PKC-μ	Fw 5'-tatccaggaaggcgtatcttgaatg-3' Rv 5'-gcctcacaccgctgcaattgtg-3'	236	60.3, 45
MMP15	Fw 5'-gtacagtggtctacttcc-3' Rv 5'-gccagtgcaagaaccac-3'	120	62.4, 40	GAPDH	Fw 5'-tggtatcggtggaaggactca-3' Rv 5'-agtgggtgctgctgttgaag-3'	371	60, 30
MMP16	Fw 5'-tgccccacaccgctctattcc-3' Rv 5'-tttcccagctcctcccacaa-3'	434	55, 45				

Table S2. MMPs and PKCs primer pairs and PCR conditions for ChIP assay

Genes	Primer pairs	Base pairs	°C, cycles	Genes	Primer pairs	Base pairs	°C, cycles
MMP1	Fw 5'-tctcctcgcacacatctg-3' Rv 5'-agcctcttgctgctccaat-3'	228	62, 40	MMP13	Fw 5'-gtgactaggaagtggaaacctatc-3' Rv 5'-caaatcatctcatcaccaccac-3'	204	62, 40
MMP2	Fw 5'-aagtggaggaggcgagta-3' Rv 5'-gtcctggcaatcccttgt-3'	211	62, 40	MMP14	Fw 5'-ggacaaagtctcccacatcc-3' Rv 5'-agtgcctccttctctggtt-3'	199	62, 40
MMP7	Fw 5'-ttgtgtcctcctccaata-3' Rv 5'-ggacctatggtgattggtgt-3'	196	62, 40	PKC-β	Fw 5'-gctgcagaatgaccaat-3' Rv 5'-gctgcgtcaggagatgt-3'	159	59, 40
MMP9	Fw 5'-tggagagaggagggtgt-3' Rv 5'-ggtgaggcagagggtgtct-3'	201	62, 40	PKC-γ	Fw 5'-ggcatcggagaaagtgagaa-3' Rv 5'-ctgcaatctgtcatcctg-3'	179	62, 40
MMP10	Fw 5'-gttgaaggaaaatactgatgtaggc-3' Rv 5'-cttcttctactggcctcta-3'	169	62, 40	PKC-θ	Fw 5'-gccattgctcaggctctaa-3' Rv 5'-ccattgataacggtggctct-3'	232	55, 40
MMP12	Fw 5'-ctctgaattccttgatgatgg-3' Rv 5'-ttagtccgggtctgtgaat-3'	152	62, 40	PKC-δ	Fw 5'-aacaggaagagcaggagtgt-3' Rv 5'-ttacagaggaggacgctga-3'	159	62, 40

Table S3. Antibodies for Western blot analysis

Antibody	Recommended dilution	Purchase from	Antibody	Recommended dilution	Purchase from
Anti-MMP1	1:5000	Bioworld	Anti-PKC-η	1:2500	Santa Cruz
Anti-MMP2	1:5000	Lab Vision	Anti-PKC-ϵ	1:10000	Santa Cruz
Anti-MMP3	1:5000	Epitomics	Anti-p21	1:10000	Epitomics
Anti-MMP9	1:5000	Lab Vision	Anti-Caspase-3	1:10000	Epitomics
Anti-MMP10	1:10000	Millipore	Anti-p-Cx43 (Ser 368)	1:5000	Santa Cruz
Anti-MMP12	1:10000	abcam	Anti-Cx43	1:2500	Santa Cruz
Anti-MMP13	1:5000	Lab Vision	Anti-p-Bcl-2 (Ser 70)	1:2500	Cell Signaling
Anti-MMP15	1:10000	Bioworld	Anti-Bcl-2	1:10000	GeneTex
Anti-PKC-α	1:10000	Epitomics	Anti-p-Bim (Ser 69)	1:2500	Cell Signaling
Anti-PKC-βI	1:5000	Abnova	Anti-Bim	1:5000	Santa Cruz
Anti-PKC-βII	1:10000	GenScript	Anti-p-P38 (Thr180/Tyr182)	1:5000	Epitomics
Anti-PKC-γ	1:10000	AVIVA Systems Biology	Anti-P38	1:10000	AnaSpec
Anti-PKC-θ	1:1000	Cell Signaling	Anti-actin	1:15000	GenScript

Figure S1.

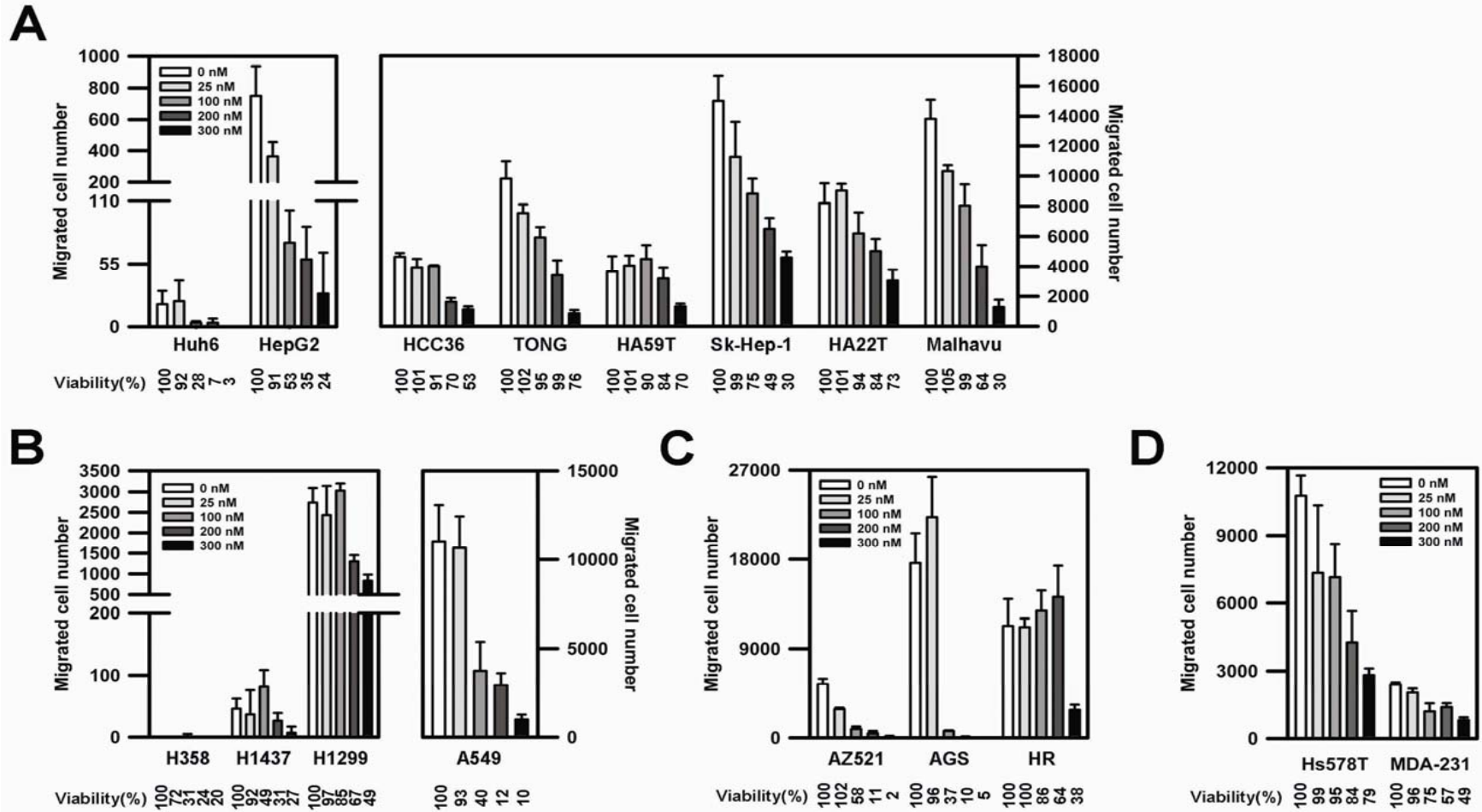


Figure S1. The remaining subset of human cancer cell lines without enhancement of cell migration activity after TSA treatment. (A) 8 HCC cell lines, (B) 4 lung, (C) 3 gastric and 2 breast cancer cell lines were treated with TSA for 24 hr and plated into TSA-contained migration chambers for transwell migration assay for another 24 hr ($n = 3$, mean \pm 95% CI). The cell viability after 48 hr TSA treatment was analyzed by alamarblue assay and represented as percentage in comparison with TSA-untreated control (100%).

Figure S2.

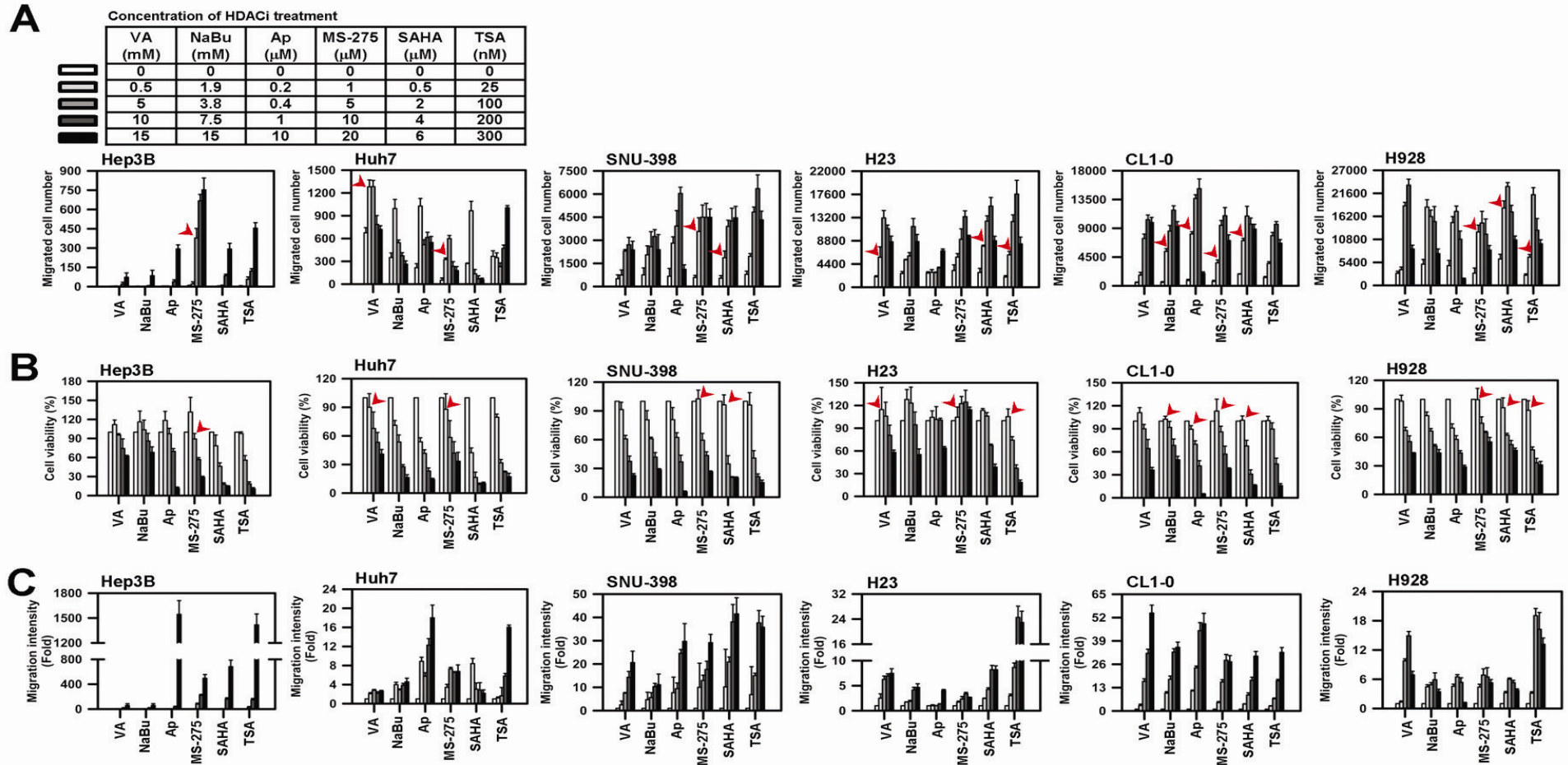
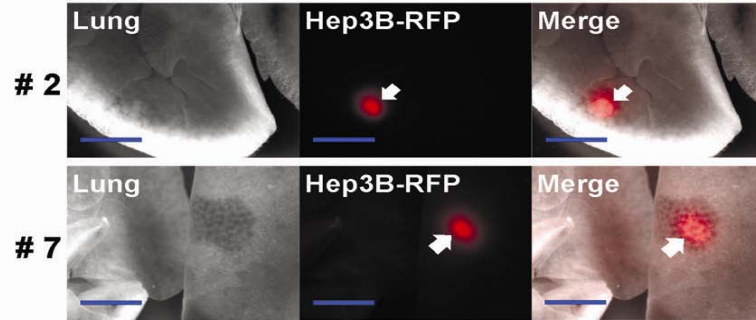


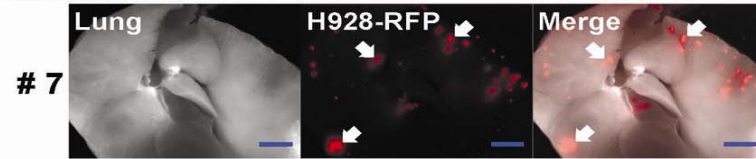
Figure S2. Validation of HDACi-enhanced cell migration with treatments of 6 different HDACi. (A) Migrated cell number in transwell migration assay of liver (Hep3B, Huh7 and SNU398) and lung (H23, CL1-0 and H928) cancer cell lines treated with various concentrations of 6 HDACi ($n = 3$, mean \pm 95% CI). (B) Cell viability of HDACi-treated cells was displayed as percentage relative to HDACi-untreated control (100%) ($n = 3$, mean \pm 95% CI). (C) Migration intensity in relative to HDACi-untreated control was calculated as fold changes ($n=3$, mean \pm 95% CI) and normalized with corresponding cell viability.

Figure S3.

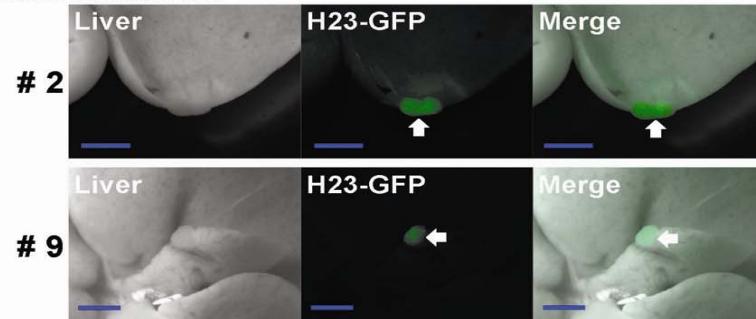
TSA treatment



VA treatment



SAHA treatment



HDACi treatments and cancer metastasis in mice

	TSA untreated mice		TSA treated mice	
	None metastasis	metastasis	None metastasis	metastasis
Hep3B injected mice	10	0	8	2
	SAHA untreated mice		SAHA treated mice	
	None metastasis	metastasis	None metastasis	metastasis
H23 injected mice	16	0	14	2
	VA untreated mice		VA treated mice	
	None metastasis	metastasis	None metastasis	metastasis
H928 injected mice	16	0	14	1
Total mice	42	0	36	5 *

* $p = 0.026$

Figure S3. HDACi treatments of HCC and lung cancer cells enhance *in vivo* experimental metastasis. In experimental metastasis assay, Hep3B-RFP, H23-GFP or H928-RFP cells were injected into mice via tail vein. One group of mice was treated with HDACi (10 mg/kg/day for TSA; 100 mg/kg/day for SAHA, and 400 mg/kg/day for VA) and the other was HDACi untreated (vehicle control mice). Metastatic cells were revealed through green or red fluorescence on lung and liver organs of mice (as indicated by arrows; scale bar, 2 mm). Table shows the summarized results and the expanded version of Table 1 (Fisher's exact test; *, $P = 0.026$).

Figure S4.

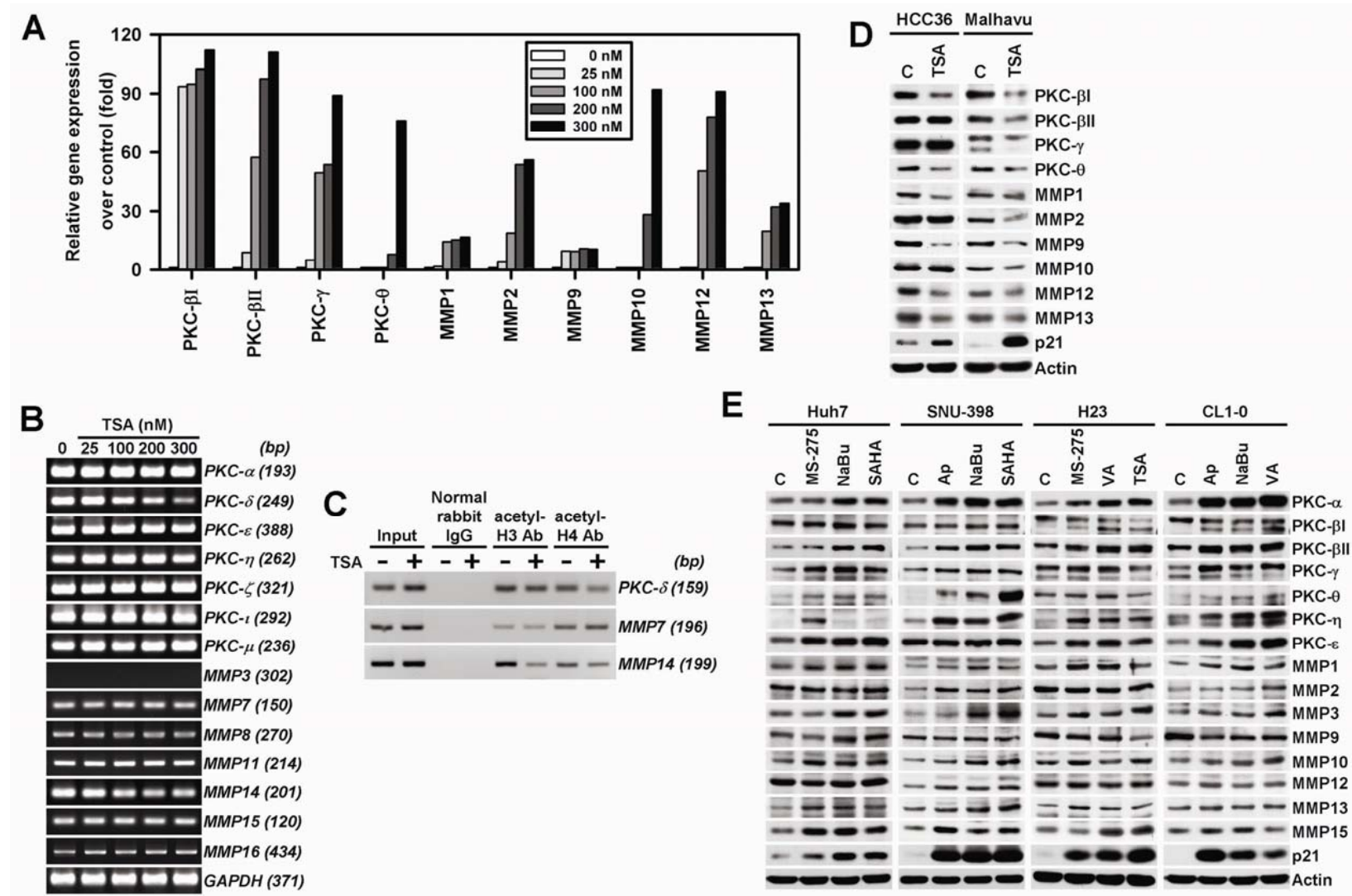


Figure S4. Treatment of HDACi modulated MMPs and PKCs expressions. (A) Quantitative bar graph of the band intensities in Figure 2A. (B) RT-PCR analysis for MMPs and PKCs expressions in TSA-treated Hep3B cells. (C) Chromatin histone H3 and H4 acetylation status of promoter regions of genes by ChIP assay in Hep3B cells. The input and normal rabbit IgG serve as loading and negative controls respectively. (D) PKCs and MMPs expressions of HCC36 and Malhavu cells can be suppressed by treated with TSA (300nM) in Western blot analysis. (E) HDACi treatments (48 hrs) up-regulated expression of members of PKCs and MMPs in Huh7 (MS-275, 5 μ M; NaBu, 1.9 mM; SAHA, 0.5 μ M), SNU-398 (Ap, 1 μ M; NaBu, 7.5 mM; SAHA, 6 μ M), H23 (MS-275, 10 μ M; VA, 5 mM; TSA, 200 nM) and CL1-0 (Ap, 1 μ M; NaBu, 7.5 mM; VA, 10 mM) cells by Western bolt analysis. Expression of p21 and actin are used as HDACi treatment and internal controls, respectively. The “C” stands for control or untreated cells.

Figure S5.

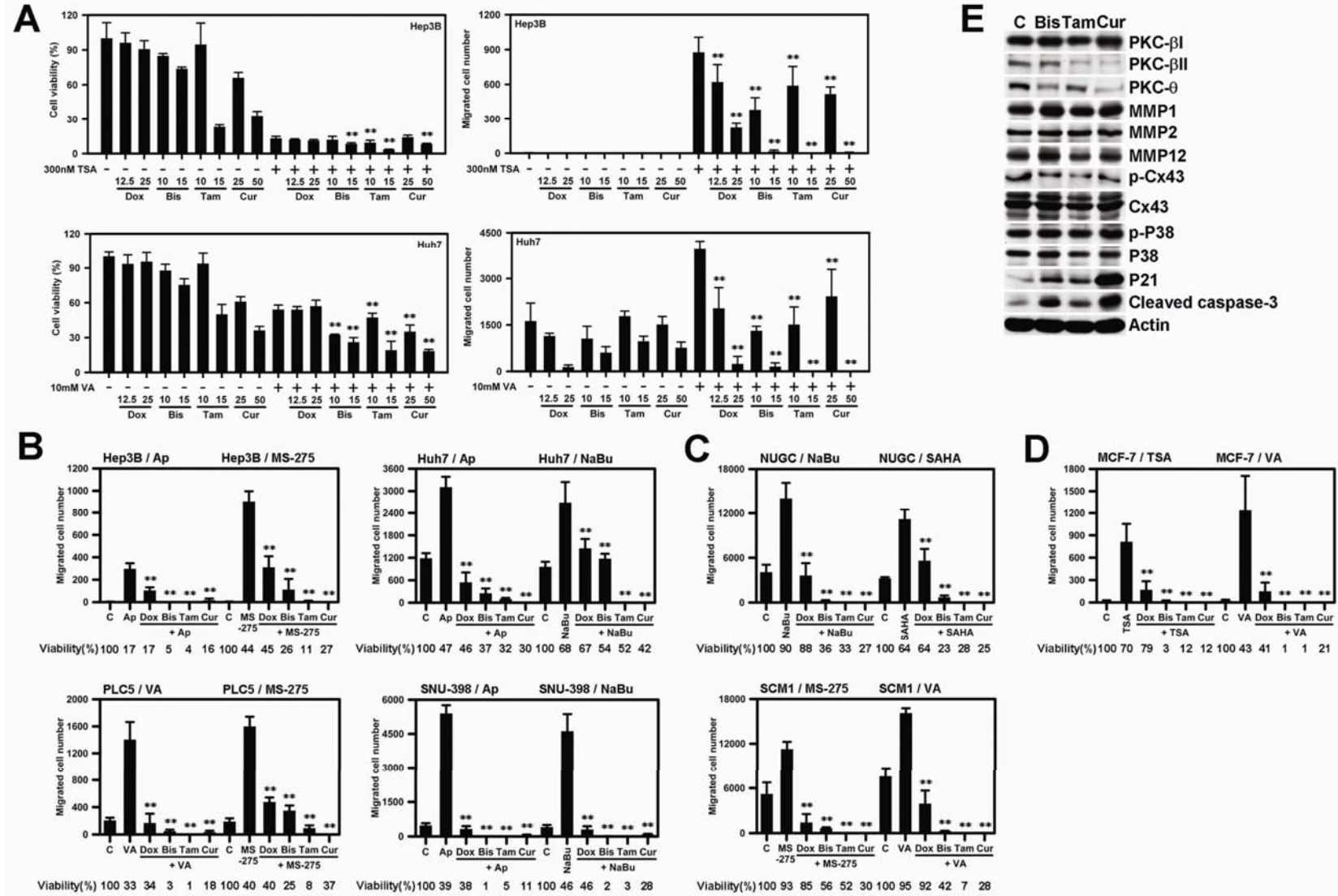


Figure S5. The combination treatments of HDACi with MMPi or PKCi repress HDACi-enhanced migration activity. (A) The cell viability and migration activity of Hep3B and Huh7 cells were analyzed after mono or combination treatments of Dox (12.5 or 25 $\mu\text{g/ml}$), Bis (10 or 15 μM), Tam (10 or 15 μM) and Cur (25 or 50 μM) with HDACi (300nM TSA or 10 mM VA). (B) HCC cells: Hep3B treated with Ap (10 μM) or MS-275 (20 μM); Huh7 treated with Ap (0.2 μM) or NaBu (1.9 mM); PLC5 treated with VA (10 mM) or MS-275 (5 μM); and SNU-398 treated with Ap (1 μM) or NaBu (7.5 mM) were conducted for combination treatments during migration assay. (C) Gastric cancer cells: NUGC treated with SAHA (2 μM) or NaBu (1.9 mM); SCM1 treated with MS-275 (1 μM) or VA (0.5 mM) were used in combined treatments with PKCi during migration assay. (D) Breast cancer cells: MCF-7 treated with TSA (100 nM) or VA (15 mM) were used in combined treatments with PKCi during migration assay. After 24 hr HDACi treatments, MMPi or PKCi including Dox (25 $\mu\text{g/ml}$), Bis (15 μM), Tam (15 μM) and Cur (50 μM) were used for HDACi combination treatments for another 24 hr during migration assay. Results were shown in migrated cell number ($n = 3$, mean \pm 95% CI). The cell viability was analyzed by alamar blue assay and displayed as percentage relative to HDACi-untreated control (100%) after 48 hr treatments ($n = 3$, mean \pm 95% CI). ** represented the significant change relative to the HDACi monotreatment ($P < 0.01$). (E) Monotreatment of Bis (15 μM), Tam (15 μM) or Cur (50 μM) can not up-regulate expressions of PKCs, MMPs and phosphorylated PKC substrate proteins of Hep3B cells in Western blot analysis. p21, cleavage form of caspase-3 and actin served as controls for HDACi treatment, cell death, and internal, respectively. The “C” stands for control or untreated cells.

Figure S6.

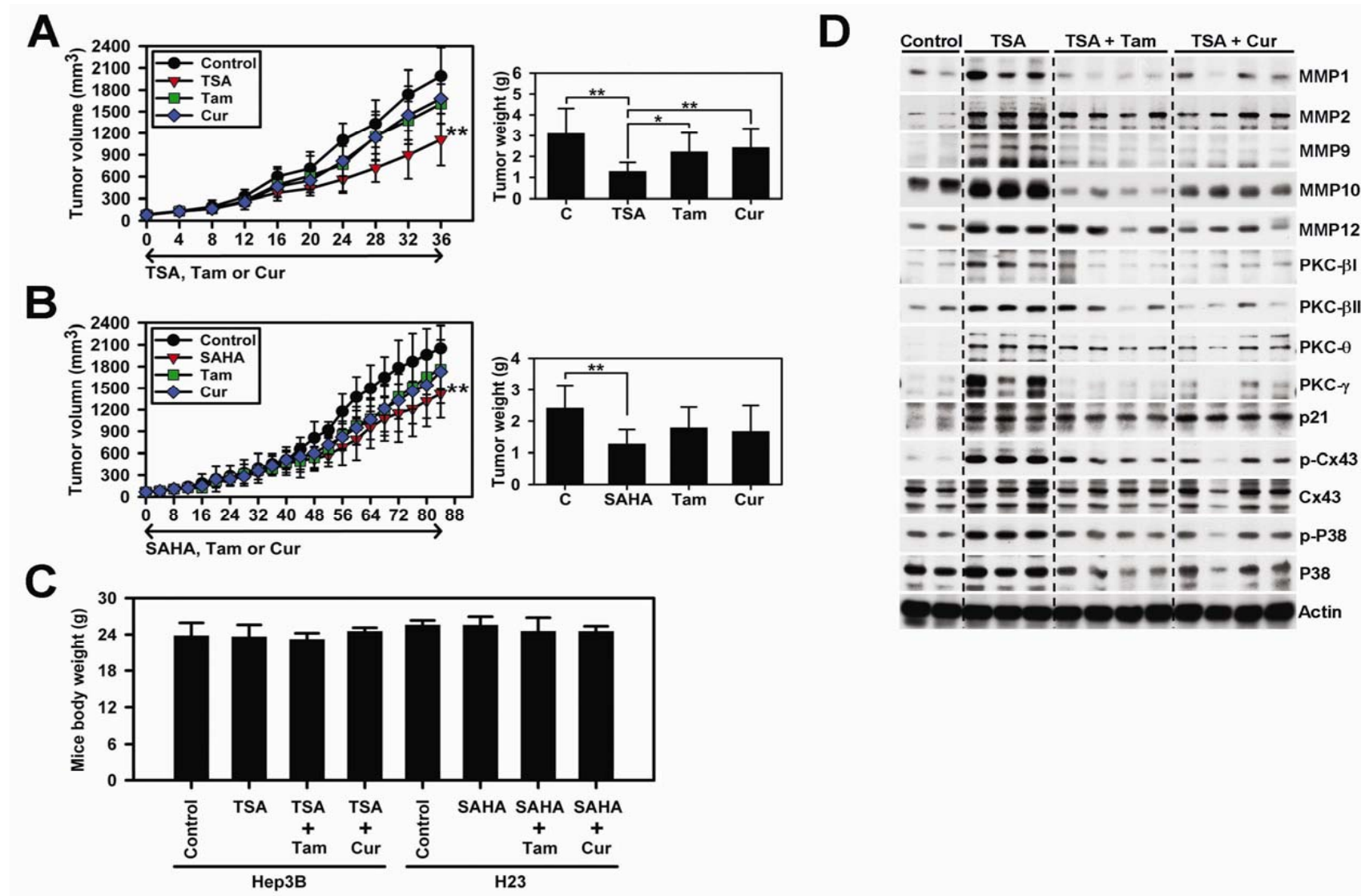


Figure S6. The effects of HDACi and PKCi on tumorigenesis, toxicity and tumor-progressive protein expressions *in vivo*.

Monotherapy of xenografted tumor models for (A) Hep3B treated with vehicle control (n = 5), TSA (n = 6, 10 mg/kg/day)-treated, Tam (n = 5, 10 mg/kg/day)-treated and Cur (n = 5, 40 mg/kg/day)-treated mice; and for (B) H23 treated with vehicle control (n = 4), SAHA (n = 5, 100 mg/kg/day)-treated, Tam (n = 5, 10 mg/kg/day)-treated and Cur (n = 5, 40 mg/kg/day)-treated mice. Tumor size was measured every 4 day and tumor weight measured after euthanasia were shown as mean \pm 95% CI (*, $p < 0.05$ and **, $p < 0.01$). (C) Combination therapies of Hep3B and H23 xenografted mice showed neither toxicity nor significant body weight changes from results of Figure 5A-5B. (D) Western blot analysis of p21, PKCs, MMPs, intracellular PKC substrates and other tumor-progressive protein expressions in Hep3B xenografted tumor tissues after combined treatments with PKCi, tamoxifen (Tam) or curcumin (Cur). Actin protein expression was internal loading control.

Figure S7.

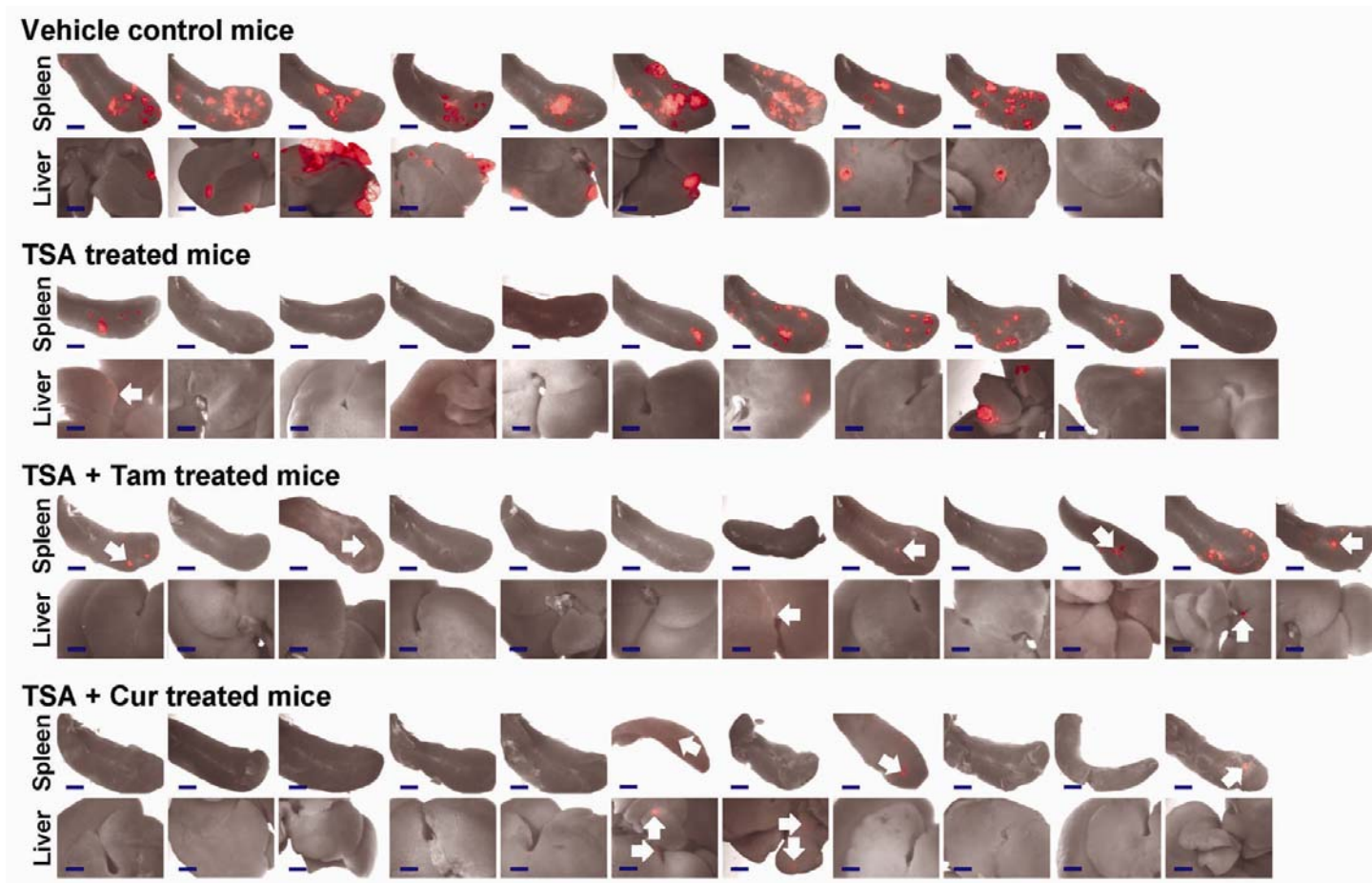


Figure S7. Suppressive effects of tumorigenesis and metastasis in liver metastasis model of TSA/Tam and TSA/Cur treated mice. Mice after intrasplenic injection with Hep3B-RFP cells were divided into 4 groups for treatments: vehicle control (n = 10), TSA (n = 11, 10 mg/kg/day)-treated, TSA/Tam (n = 12, 10 mg/kg/day)-treated and TSA/Cur (n = 11, 40 mg/kg/day)-treated mice. Tumors on spleen and liver metastasis were revealed by red fluorescence (scale bar, 2 mm).